Supplementary information for "Influence of bacterial swimming and hydrodynamics on attachment of phages"

Christoph Lohrmann* and Christian Holm†
Institute for Computational Physics, University of Stuttgart, 70569 Stuttgart, Germany

Sujit S. Datta‡
Department of Chemical and Biological Engineering, Princeton University, Princeton, New Jersey 08544, USA

(Dated: May 31, 2024)

I. FAR FIELD DECAY OF THE SWIMMING FLOW FIELD

In Figure S1 we show the decay of the flow field $\langle|\mathbf{v}_{\text{fluid}}|\rangle_\Theta(r)$ generated by the swimming bacterium. Here, $\langle\cdot\rangle_\Theta(r)$ refers to an average over all angles Θ at distance r from the center location between the cell body and flagellar bundle. Numerically, these values are obtained from linear interpolation of the lattice Boltzmann grid. We fit a power law function $f(r) = a \cdot r^\alpha$ to obtain the exponent α governing the leading order behaviour far from the cell. Our simulations yield $\alpha = -2.12(3)$, which is very close to the theoretically expected exponent $\alpha^{\text{dipole}} = -2$, showing that our model captures the swimming flow field well.

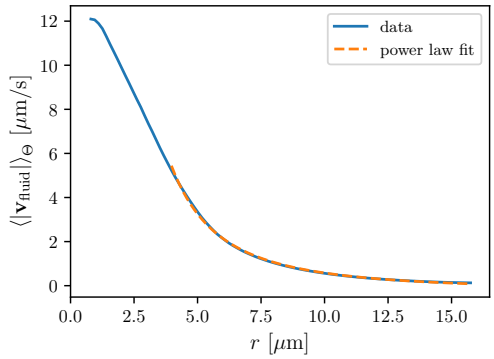

[H]

FIG. S1. Angle-averaged flow field around the swimmer as a function of distance. The power law fit yields a far-field exponent $\alpha = -2.12(3)$.

* clohrmann@icp.uni-stuttgart.de
† holm@icp.uni-stuttgart.de
‡ ssdatta@princeton.edu

II. BACTERIUM AND PHAGE MODEL CALIBRATION

Figure S2 shows that using our choice of $\tilde{\gamma}$ and determining the corresponding effective mobility leads to the desired swim speed of the bacterium. In Fig. S3 we show that applying the grid correction to γ^P leads to the correct diffusion coefficient of the phages.

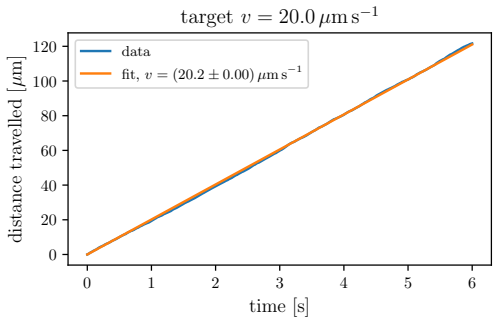

FIG. S2. Bacterium distance travelled and swim speed fit.

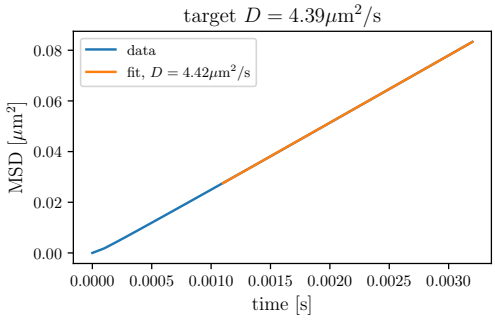

FIG. S3. Phage mean squared displacement and diffusion coefficient fit.

III. DETERMINATION OF ATTACHMENT RATE

Figure S4 shows exemplary encounter data for a single simulation and the fit that is used to determine the

attachment rate.

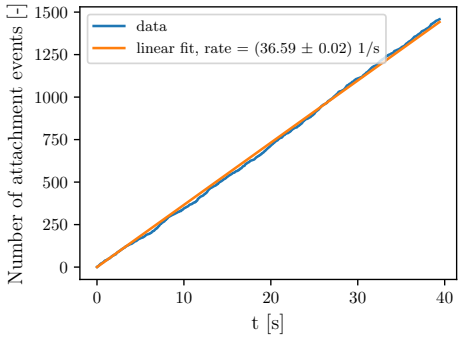

FIG. S4. Number of attachment events vs time for one simulation with hydrodynamics, $k^{\mathrm{att}} \to \infty$ and $v_{\mathrm{swim}} = 100\,\mu\mathrm{m\,s}^{-1}$

IV. EXCLUSION OF FINITE SIZE AND DENSITY EFFECTS

In Fig. S5 we show that the attachment rate is independent of the box size and independent of the phage number density.

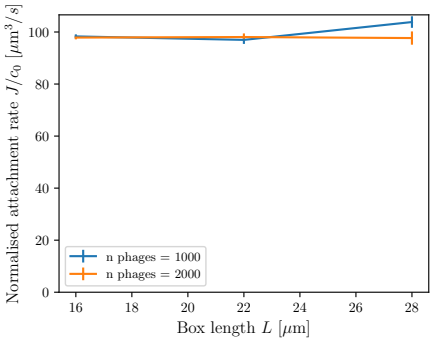

FIG. S5. Attachment rate as a function of simulation box length for different numbers of phages. Simulations performed with hydrodynamics at $v_{\mathrm{swim}} = 25\,\mu\mathrm{m\,s}^{-1}$ and $k^{\mathrm{att}} \to \infty$.

In Fig. S6 we show that the phage mass density increase has no influence on the attachment rate. There is no appreciable difference in the results between a mass density increase of 1×10^5, which is the value used in the study, and 5×10^4. Only for larger densities, the influence of momentum becomes relevant.

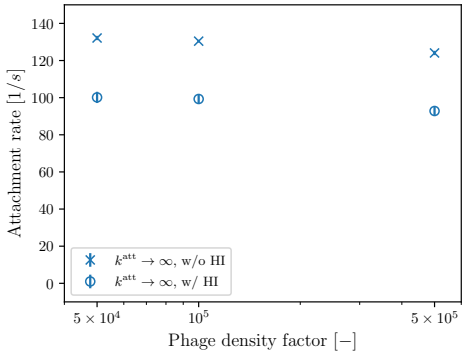

FIG. S6. Attachment rate as a function of phage mass density increase factor. Simulations performed at $v_{\mathrm{swim}} = 25\,\mu\mathrm{m\,s}^{-1}$.

V. DESCRIPTION OF SI MOVIE

`simulation_setup.mp4`: A pusher bacterium swimming at velocity $v_{\mathrm{swim}} = 25\,\mu\mathrm{m\,s}^{-1}$ in a periodic simulation box of dimension $(25\,\mu\mathrm{m})^3$ with 100 phages. The size of the phages is increased by a factor of 3 for better visibility.

VI. ATTACHMENT PROBABILITY DENSITIES

Figure S7 shows probability densities of phage attachment locations in addition to the one exemplary case in the main text.

VII. FINITE k^{att}

Figures S8 and S9 show the results for attachment rate and location on the body and flagellum, respectively. The data for $k^{\mathrm{att}} \to 0, \infty$ are the same as in the corresponding figures in the main text. For intermediate k^{att}, the curves show the same qualitative behaviour as in the two limiting cases.

VIII. PULLER SWIMMERS

Figures S10 and S11 show results for attachment rate and position for the body and flagellum, respectively. To obtain this data, puller type swimmers with the flagellum in front of the cell body were simulated.

Phages in the swimming direction are taken up by the flagellum before they can reach the front of the cell body. Therefore, in simulations without hydrodynamics, the main mechanism of attachment rate increase on the cell body – uptake of more phages in the front – is strongly reduced. As a result, the attachment rate increase is

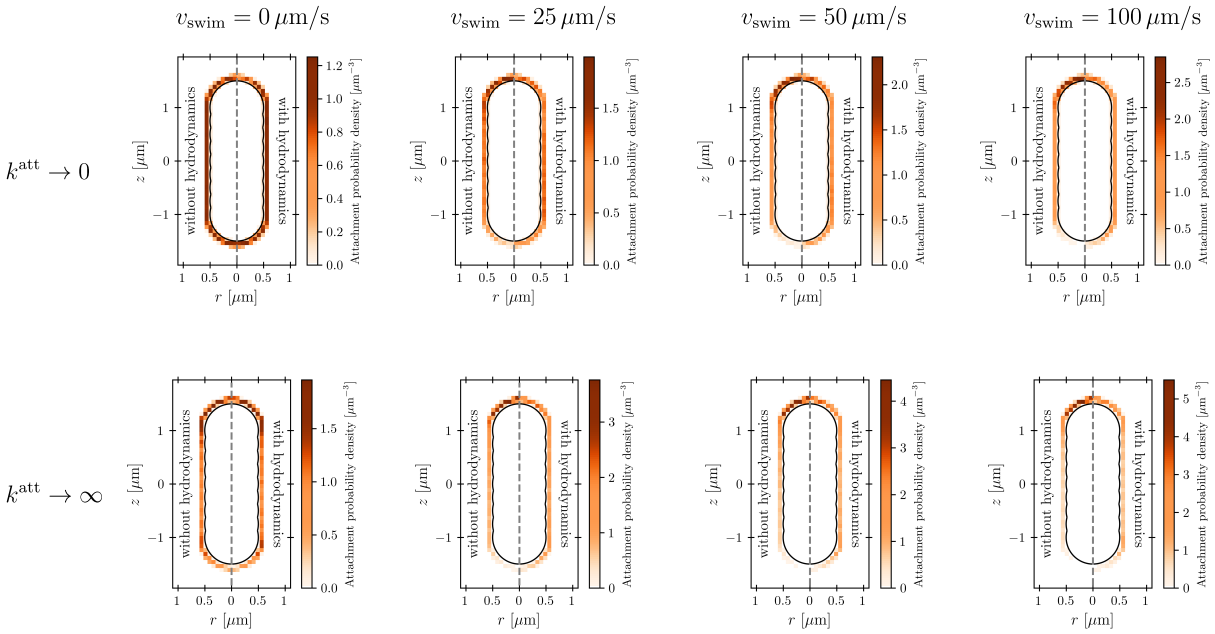

FIG. S7. Probability distribution of phage attachment locations on the cell body analogous to Fig. 5 of the main text.

much smaller than for pushers and is also not captured by the cross sectional model.

When hydrodynamic interactions are considered, there is almost no increase in attachment rate on the cell body regardless of k^{att}. For the pusher, the attachment rate increases with v_{swim} because the region with $\mathrm{Pe}^*_{\mathrm{Phage}} < 1$ shrinks around the forward end of the cell body and phages have to cross less distance by diffusion. For the puller, the shape of $\mathrm{Pe}^*_{\mathrm{Phage}} < 1$ around the forward end of the cell body is roughly independent of the swim speed as it is mainly determined by the details of the gap between cell surface and the propelling part of the flagellum. Therefore, the only increase of attachment rate comes from phages that arrive from the sides, leading to the small influence of motility. Unsurprisingly, the model of Berg et al. cannot be employed for puller bacteria and flagellotropic phages, because now the flagellum is the main collector of phages instead of the cell body.

The dependence of the attachment location on the cell body is qualitatively the same as in the pusher case, except that the curves are shifted to negative values at $v_{\mathrm{swim}} = 0$ because of the sink of phage concentration now in front of the cell body.

For the flagellum, the qualitative observations and explanations for the behavior of attachment rate and location are the same as in the pusher case.

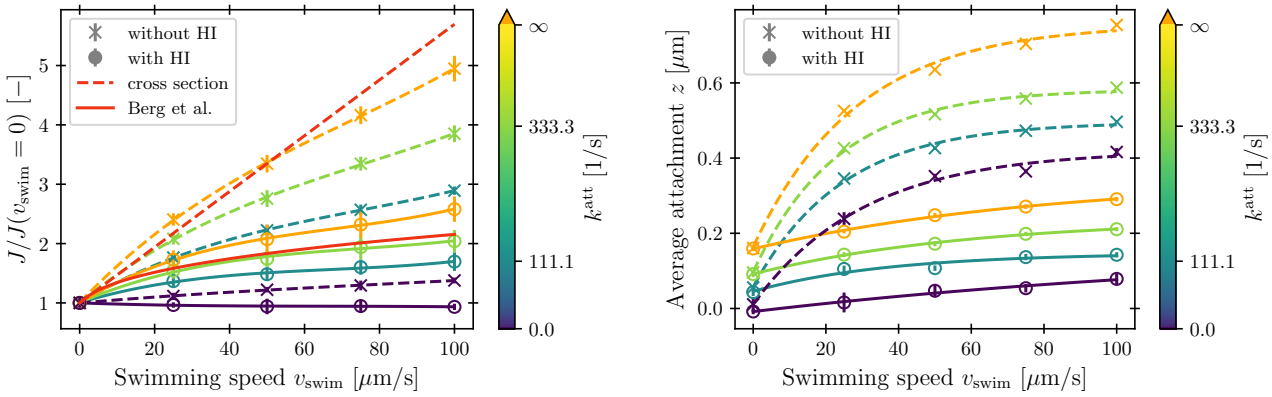

FIG. S8. **Pusher** bacterium: Attachment rate and positions on the **cell body** for finite k^{att}. Polynomial/exponential fits are shown to guide the eye.

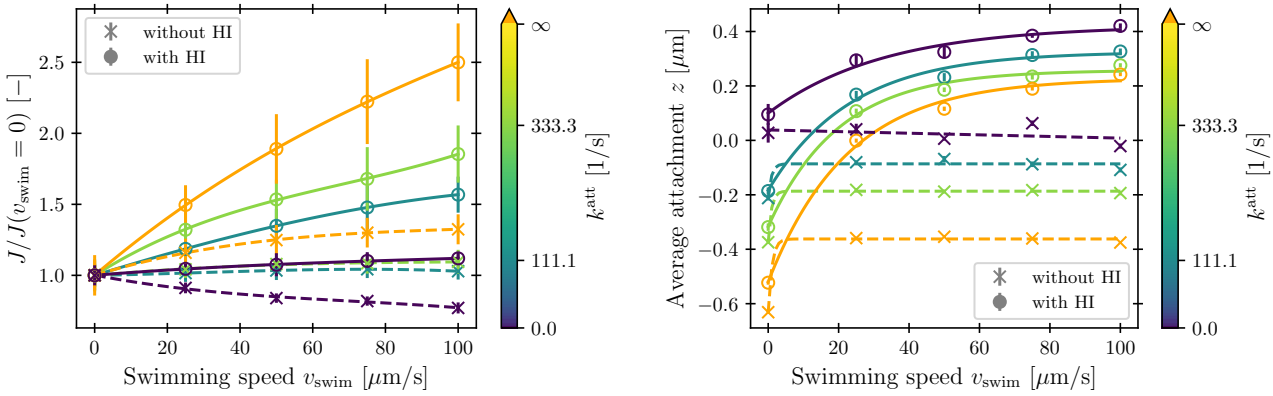

FIG. S9. **Pusher** bacterium: Attachment rate and positions on the **flagellum** for finite k^{att}. Polynomial/exponential fits are shown to guide the eye.

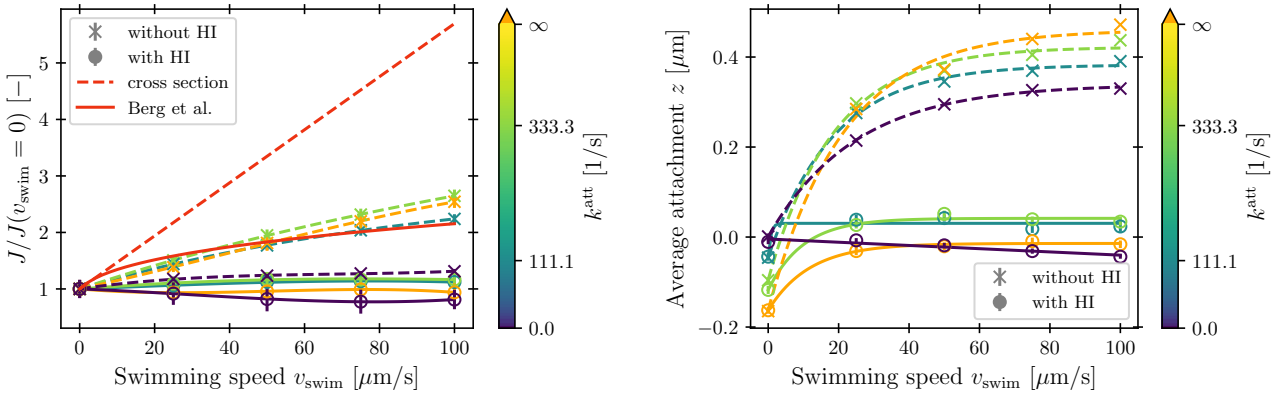

FIG. S10. **Puller** bacterium: Attachment rate and positions on the **cell body** for finite k^{att}. Polynomial/exponential fits are shown to guide the eye.

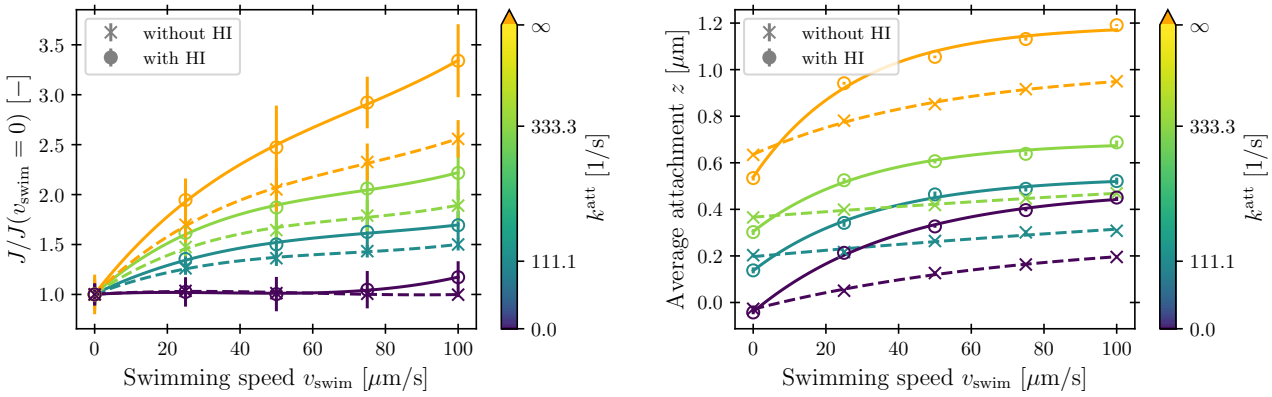

FIG. S11. **Puller** bacterium: Attachment rate and positions on the **flagellum** for finite k^{att}. Polynomial/exponential fits are shown to guide the eye.